



BOX WING FUNDAMENTALS – AN AIRCRAFT DESIGN PERSPECTIVE

D. Schiktanz, D. Scholz
Hamburg University of Applied Sciences
Aero – Aircraft Design and Systems Group
Berliner Tor 9, 20099 Hamburg, Germany

Abstract

A systematic and general investigation about box wing aircraft is conducted, including aerodynamic and performance characteristics. The design of a promising medium range box wing aircraft based on the Airbus A320 taken as reference aircraft is performed. The design is taken through the general steps in aircraft preliminary design. The fuel consumption of the final aircraft is 9 % lower than that of the reference aircraft. The aircraft layout is well balanced regarding the position of the center of gravity and the travel of the center of gravity is minimized. This is necessary due to the aircraft's particular characteristics concerning static longitudinal stability and controllability. The low wing tank capacity requires an additional fuselage tank. Because of its high span efficiency the aircraft has a glide ratio of 20,4. Its wing is about twice as heavy as the reference wing. This is partly compensated by a lighter fuselage.

1. INTRODUCTION

1.1. Motivation

A promising configuration for future aircraft is the box wing configuration (see FIG. 1) which assures savings in fuel consumption compared to conventional aircraft. These savings come from a reduction of induced drag resulting in a higher glide ratio. Facing the demand of a 75 % reduction of CO₂ emissions and a 90 % reduction of NO_x emissions formulated in [1] future aircraft have to be more efficient. These goals may be accomplished through better technologies, lighter materials and alternative fuels. The box wing configuration allows to save fuel already because of its superior aerodynamics, thus the aircraft configuration contributes to reach the goals of [1]. This is not the case for today's conventional configurations.

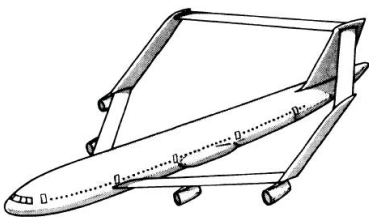


FIG. 1 Example of a box wing aircraft [2]

In order to understand the box wing configuration it has to be agreed on clear definitions of terms. These definitions seem to lack in other related publications. Once they are set up it is easier to determine the design parameters of an actual box wing aircraft and to assess its performance. In this paper a medium range box wing aircraft is presented evolving from fundamental investigations regarding the unconventional qualities of the configuration. These fundamentals are presented as well in order to give a summary of the characteristics which distinguish the box wing from a conventional configuration in the perspective of aircraft design.

This paper was conducted within the research project Airport 2030 [3]. The designed medium range box wing aircraft is supposed to provide answers on how to reduce emissions in the airport environment and how to reduce costs for airlines with the help of an unconventional and more efficient aircraft.

1.2. Objectives and Structure of this Paper

One aim of this paper is to give a summary of geometric definitions of the box wing configuration which are necessary to determine its aerodynamic characteristics. It presents methods on how to assess the induced drag of the configuration depending on its geometry. This makes it possible to determine the span efficiency factor as well. Next the lift curve slope is discussed including the effects of downwash of the forward wing on the aft wing. The relating consequences on aircraft performance are investigated, too. This includes general considerations concerning the glide ratio and the cruise altitude. Another topic is the design of the wing configuration which reveals several critical aspects like the wing weight, the volume of the wing tanks as well as the design for transonic speeds, optimum aerodynamics and for meeting stability requirements. At last the requirements gathered with the help of these fundamental investigations are applied to the design of a medium range box wing aircraft. It is described in which way they are put into practice. The performance of the derived aircraft is evaluated in order to assess the potential of the box wing configuration more thoroughly.

1.3. Definitions

CG Envelope

The CG envelope is the permissible region for the aircraft's center of gravity for all flight and ground operations.

Reference Aircraft

For evaluating the performance of a box wing aircraft it is necessary to define a reference aircraft the box wing

aircraft is based on (Airbus A320). Both aircraft have the same design mission which allows for comparing their performance. For a clear comparison both aircraft have the same wing span and total wing reference area. The data for the reference area is taken from published information and from [4].

Reference Mission

It comprises a range of 1550 nm for a payload of 20 t. The cabin is supposed to accommodate 150 passengers in a two class layout. The cruise Mach number is 0,76. The take off field length is 2200 m and the landing field length is 1700 m.

Reference Wing

The reference wing is the wing of the reference aircraft.

2. GEOMETRY DEFINITIONS

2.1. Aspect Ratio

2.1.1. Whole Wing Configuration

The main feature of the box wing configuration is its low induced drag, whose coefficient is commonly expressed by (1):

$$(1) C_{D,i} = \frac{C_L^2}{\pi \cdot A \cdot e}$$

In order to calculate the induced drag coefficient of the box wing aircraft it is necessary to know its aspect ratio and its span efficiency factor. The approach used in the current study is to define the aspect ratio of the whole wing configuration and to use this definition for the determination of the span efficiency factor with the help of published data concerning the induced drag of box wings.

The designed medium range box wing aircraft is supposed to have wings with equal spans. For this case [5] gives a definition of the total aspect ratio. It is the span of the wings squared divided by the sum of the individual wing areas:

$$(2) A = \frac{b^2}{S_1 + S_2} = \frac{b^2}{S}$$

Provided that the wing of a conventional reference aircraft is split into the two wings of the box wing aircraft and assuming that the total wing area as well as the wing span remain the same, the reference aspect ratio is equal to the box wing aspect ratio.

Of course it is possible to have different spans of both wings of the box wing aircraft which would make it necessary to adapt the definition of the aspect ratio. However, this case is not considered in this paper.

2.1.2. Individual Wings

Applying the final term of (2) to an isolated wing of the box wing aircraft results in an aspect ratio double the aspect ratio of the whole configuration, assuming that there is an equal split of the total wing area between both wings.

According to (1) the induced drag of an isolated wing is then reduced because of the higher aspect ratio. Yet this approach might be misleading, since wing interference effects are not taken account of.

2.2. Mean Aerodynamic Chord

The mean aerodynamic chord (MAC) is usually used to express the travel of the aircraft's center of gravity (CG) in terms of % MAC. The longitudinal position of the MAC is necessary to determine the lever arm between the tail surfaces and the wing configuration for sizing the tail surfaces and for assessing the aircraft's stability characteristics.

2.2.1. Length

For a conventional wing the length of the MAC is determined with

$$(3) \bar{c} = \frac{2}{S} \int_0^{b/2} c(y)^2 dy$$

When neglecting the vertical winglets the box wing consists of two conventional wings, so (3) can be used to calculate \bar{c} for each wing separately. Now the length of the total MAC can be calculated with the help of \bar{c}_1 and \bar{c}_2 :

$$(4) \bar{c} = \bar{c}_1 \cdot s_1 + \bar{c}_2 \cdot s_2 \quad \text{with}$$

$$(5) s_1 = \frac{S_1}{S_1 + S_2} \quad \text{and}$$

$$(6) s_2 = \frac{S_2}{S_1 + S_2}$$

(4) also applies to a double trapeze wing. The parameters with the index 1 would be those of the inner trapeze and the parameters with the index 2 those of the outer trapeze. The derivation of (4) in connection with a box wing aircraft can be found in [6].

2.2.2. Longitudinal Position

The method for determining the longitudinal position of the MAC is based on the moments and forces generated by both wings which generate a total pitching moment. The substitute wing the MAC is based on is supposed to generate the same total pitching moment. This correlation is depicted in FIG. 2 with the help of an arbitrary box wing aircraft.

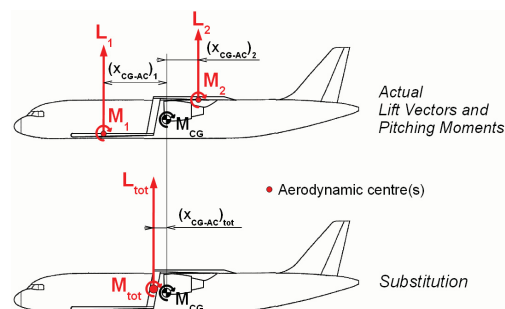


FIG. 2 Lift forces and pitching moments acting on the wings and their substitution

Building the equilibrium of moments about the CG according to the actual lift vectors and pitching moment gives

$$(7) \quad M_{CG} = M_1 + L_1(x_{CG-AC})_1 + M_2 + L_2(x_{CG-AC})_2.$$

Doing the same based on the substitute wing yields

$$(8) \quad M_{CG} = M_{tot} + L_{tot}(x_{CG-AC})_{tot} \quad \text{where}$$

$$(9) \quad M_{tot} = M_1 + M_2 \quad \text{and}$$

$$(10) \quad L_{tot} = L_1 + L_2.$$

The longitudinal MAC position in terms of the distance to the aircraft's CG is expressed by $(x_{CG-AC})_{tot}$. In fact this is the position of the aerodynamic center of the wing configuration, which in turn is assumed to be at 25 % MAC. Combining (7), (8), (9) and (10) and substituting for $(x_{CG-AC})_{tot}$ finally results in

$$(11) \quad (x_{CG-AC})_{tot} = \frac{L_1(x_{CG-AC})_1 + L_2(x_{CG-AC})_2}{L_1 + L_2}.$$

Note the opposite algebraic signs of $(x_{CG-AC})_1$ and $(x_{CG-AC})_2$.

2.3. Stagger

The horizontal distance between both of the wings is referred to as stagger. The concept of staggering wings was already applied to the design of simple biplanes. Different stagger means different interactions between both wings. For each amount of stagger it is possible to establish the optimum lift distribution by applying accordant wing twist and taper. This is known as Munk's stagger theorem.

There is the distinction between positive and negative stagger. The wing configuration shown in FIG. 3 has positive stagger.

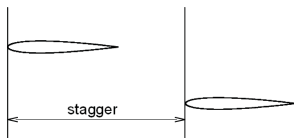


FIG. 3 Positive stagger of a biplane

Whether the amount of stagger is determined based on the individual MACs or any other geometric property (e.g. the root positions) depends on the purpose.

2.3.1. Height/Gap

"Gap" is mostly referred to as the height of the wing configuration. It is usually expressed with the help of the height to span ratio h/b which is a characteristic feature of non planar configurations. It is the parameter which mostly influences the induced drag of the wing configuration. In [2] and [7] it is said that the crucial distance is the gap at the wing tips, hence the ratio h_i/b .

3. BOX WING AERODYNAMICS AND PERFORMANCE

In this section not every single aspect is considered, but those whose characteristics are significantly different compared to conventional configurations.

3.1. Lift Distribution

The optimum lift distribution for minimum induced drag of the box wing configuration consists of a constant and an elliptical part for the horizontal wings and a linear and butterfly shaped part for the vertical wings ([8], FIG. 4). This fact is also confirmed by more recent studies performed in [9].

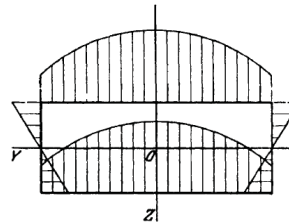


FIG. 4 Lift distribution of a box wing aircraft [8]

Judging from literature there seems to be some controversy about which additional conditions are necessary for minimum induced drag. In [2] and [10] general biplane theory is used which states that both wings have to generate the same amount of lift. However, in [11] and [12] it is suggested that a constant circulation loop can be added to the overall distribution which leads to unequal lift of both wings without an increase of induced drag. In this case there are different constant parts at both wings while their elliptical parts are still equal. This leads to a shift of the zero crossing of the winglet loading and also to a heavy tip loading of the wing which generates more lift (FIG. 5).

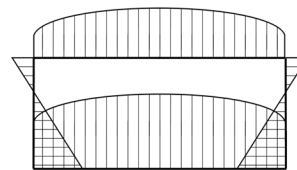


FIG. 5 Lift distribution with unequal lift for both wings

For the design of the medium range box wing aircraft the additional condition according to biplane theory is used. With the help of ongoing aerodynamic studies it is investigated if lift distributions as shown in FIG. 5 also lead to minimum induced drag.

3.2. Induced Drag

The box wing configuration is known for its low induced drag, as all non planar configurations. In this section simple methods of justifying the savings in induced drag are proposed. They do not claim to reflect the exact aerodynamics but give statements from the perspective of aircraft design.

It is possible to analyze the individual wings isolated or to treat the wing configuration as a whole.

3.2.1. Isolated Wings

(12) is used to compare the total induced drag of a box wing configuration with that of a conventional reference aircraft with the same wing span.

$$(12) D_i = \frac{L^2}{q \cdot \pi \cdot b^2 \cdot e}$$

For the beginning it can be assumed that one wing of the box wing configuration carries half of the total lift and that the dynamic pressure is the same for all wings. So building the ratio of the induced drag of one isolated wing of the box wing aircraft and that of the reference wing gives

$$(13) \frac{(D_{i,box})_{iso}}{D_{i,ref}} = \left(\frac{1}{2}\right)^2 \cdot \frac{e_{ref}}{(e_{box})_{iso}}$$

Provided that $(e_{box})_{iso} = e_{ref}$ the induced drag of one isolated wing of the box wing aircraft would be quarter the induced drag of the reference wing. Since the box wing aircraft has two wings, it would be:

$$(14) \frac{D_{i,box}}{D_{i,ref}} = 0,5$$

However, this result is very optimistic because it does not take account of the mutual interferences between both wings of the box wing aircraft. The interferences cause that $(e_{box})_{iso} < e_{ref}$, which in turn leads to $D_{i,box}/D_{i,ref} > 0,5$. A value of 0,5 applies to an infinite gap between both wings. In this case possible effects caused by the winglets are neglected. The determination of $(e_{box})_{iso}$ requires profound aerodynamic analysis. Within the scope of aircraft design it is sufficient to regard the wing configuration as a whole and to determine the span efficiency e_{box} of the whole wing configuration.

3.2.2. Whole Wing Configuration

Applying (12) for a comparison of the whole wing configuration of both the box wing and the reference aircraft gives

$$(15) \frac{D_{i,box}}{D_{i,ref}} = \frac{e_{ref}}{e_{box}}$$

Here it is assumed that both aircraft have the same weight, the same wing span and are exposed to the same dynamic pressure.

The term $D_{i,box}/D_{i,ref}$ can be taken from published data and is a function of the h/b ratio. This way it is possible to calculate the span efficiency of the box wing configuration which is needed for the preliminary sizing of the aircraft. For doing so the span efficiency of the reference aircraft is required.

It is important not to mix the characteristics of the isolated wings of the box wing aircraft with those of the whole wing configuration. As shown it is possible to identify the trend

of reduction of induced drag by treating the wings as isolated. But in this case it is difficult to assess the actual induced drag in a satisfactory manner. However, this is possible by treating the wing configuration as a whole since enough data has been published serving (15). A summary of these data is given in section 3.2.3 together with a recommendation of the most suitable approach.

3.2.3. $D_{i,box}/D_{i,ref}$ from Literature

The data from three sources, namely [13], [14] and [9] are compared.

In general the ratio of induced drag is expressed as function of the h/b ratio and accounts for ideally loaded wings. The general form of the found equations is

$$(16) \frac{D_{i,box}}{D_{i,ref}} = f(h/b) = \frac{k_1 + k_2 \cdot h/b}{k_3 + k_4 \cdot h/b}$$

With the help of several investigations it was tried to adapt the free parameters k_1, k_2, k_3 and k_4 so that the results resemble measured or calculated data. The first approach was published in [13] and reads

$$(17) \frac{D_{i,box}}{D_{i,ref}} = \frac{1 + 0,45 \cdot h/b}{1,04 + 2,81 \cdot h/b}$$

When h/b tends to infinity (17) gives 0,16. This is far below the value predicted in section 3.2.1.

From a more recent study published in [14] the following equation was taken:

$$(18) \frac{D_{i,box}}{D_{i,ref}} = \frac{0,44 + 0,9594 \cdot h/b}{0,44 + 2,219 \cdot h/b}$$

It was determined by using CFD and thus includes numerical errors. Its limit value is about 0,43 which seems more realistic compared to the value coming from (17).

In [10] a graph is presented which includes an exact solution for the induced drag of a box wing configuration depending on the h/b ratio. The solution was published in [9] and is based on an analysis of the distribution of circulation along the individual wings. The derived relations were evaluated through numerical methods. This is why no equation in the form of (16) was formulated. Only the graph is available (FIG. 6).

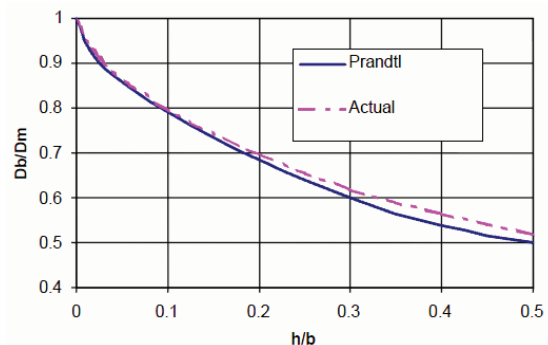


FIG. 6 Comparison of results from Prandtl (17) and Frediani [9]; published in [10]

It can be seen that the results according to (17) are too optimistic. For the sake of comparison the correlation for a normal biplane is given as well, coming from [13]:

$$(19) \frac{D_{i,bi}}{D_{i,ref}} = 0,5 + \frac{1 - 0,66 \cdot h/b}{2,1 + 7,4 \cdot h/b}$$

The limit value of (19) is about 0,41, which resembles the limit value of (18).

FIG. 7 shows a plot of (17), (18) and (19).

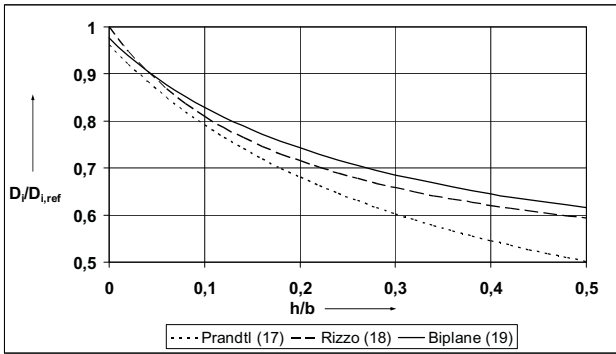


FIG. 7 Comparison of results from (17), (18) and (19)

It was already mentioned that (17) overestimated the efficiency of a box wing configuration. (18) comes close to the results of a simple biplane. The exact solution from [9] shown in FIG. 6 would be in between the graphs for (17) and (18). Considering the fact that no plain equation exists for the exact solution and choosing a more conservative approach for meeting concerns because of the complex box wing aerodynamics and since compressibility is neglected in this study, (18) is used for the design of the medium range box wing aircraft.

3.2.4. Resulting Span Efficiency Factor

According to (15) and with the results of (18) the span efficiency factor of the box wing configuration can be determined. The resulting equation is

$$(20) e_{box} = e_{ref} \cdot \frac{0,44 + 2,219h/b}{0,44 + 0,9594h/b}$$

In [15] the span efficiency factor of a conventional aircraft is estimated to be 0,85 for cruise and 0,7 for landing. These values are used for e_{ref} .

3.3. Lift Curve Slope

The lift curve slope is important for predicting the angle of attack where stall is to be expected as well as the angle of attack for all flight phases. It also influences the reaction of the aircraft to gusts. As for the analysis of induced drag it has to be differentiated between the characteristics of the isolated wings and those of the whole wing configuration.

3.3.1. Isolated Wings

According to [15] the lift curve slope of a wing can be estimated with

$$(21) \frac{dC_L}{d\alpha} \approx \frac{2 \cdot \pi \cdot A}{2 + \sqrt{A^2 \cdot (1 + \tan^2 \varphi_{s0} - M^2)} + 4}$$

Supposing that both the reference wing and the box wing have a sweep of 25° and neglecting effects of compressibility, the ratio of lift curve slopes of the reference wing and the box wing can be calculated:

$$(22) \frac{(dC_L/d\alpha)_{box,iso}}{(dC_L/d\alpha)_{ref}} = \frac{2 \left(2 + \sqrt{A_{ref}^2 \cdot (1 + \tan^2 25^\circ)} + 4 \right)}{2 + \sqrt{4A_{ref}^2 \cdot (1 + \tan^2 25^\circ)} + 4} = 1,10.$$

(22) includes the assumption that $A_{ref} = 0,5A_{box,iso} = 9,5$. So because of the higher aspect ratio the lift curve slope of a single wing is increased by 10%. This does not include any interference effects, more precisely downwash. It is considered in the next section.

3.3.2. Whole Wing Configuration

A simple equation for the total lift curve slope of two lifting surfaces can be derived from [16]. It reads

$$(23) \frac{dC_L}{d\alpha} = \frac{dC_{L,1}}{d\alpha} \cdot s_1 + \frac{dC_{L,2}}{d\alpha} \cdot s_2 \cdot \left(1 - \frac{d\varepsilon}{d\alpha} \right).$$

So the contribution of the aft wing to the total lift curve slope is lowered because of the downwash of the forward wing. The isolated lift curve slopes can be determined with the help of (21). In the beginning it is assumed that $s_1 = s_2 = 0,5$ and $dC_{L,1}/d\alpha = dC_{L,2}/d\alpha$. Provided a downwash gradient of about 0,1 the overall lift curve slope of the box wing aircraft is reduced by 5% compared to that of the isolated wings. Transferring this to the result of (22) results in a ratio of lift curve slopes of about 1,05.

Strictly speaking (23) only applies to configurations where the span of the aft surface is significantly smaller than that of the forward surface. But (23) is sufficient for roughly assessing the downwash effect on the lift curve slope. A more detailed analysis taking account of equal spans of both lifting surfaces was conducted in [6]. There it is found that by using (23) the lift curve slope of the box wing configuration is slightly overestimated.

Note that the current analysis of the lift curve slope does not consider interference effects between the wings and the vertical winglets. From [17] it can be understood that these interferences additionally increase the total lift curve slope, so the ratio of 1,05 derived here probably is too small. The interferences are not considered in [6] as well.

3.4. Individual Lift Coefficients and Total Lift Coefficient

In general the total lift coefficient depending on the lift coefficients of the individual wings is calculated with

$$(24) C_L = C_{L,1} \cdot s_1 + C_{L,2} \cdot s_2$$

The lift coefficient depending on the lift curve slope is

$$(25) C_L = \frac{dC_{L,i}}{d\alpha} \cdot \alpha,$$

where α is the angle of attack with regard to the zero lift line. Using (25) for the determination of the individual lift coefficients in (24) and taking account of the downwash results in

$$(26) C_L = \left[\frac{dC_{L,1}}{d\alpha} \right] \cdot s_1 + \left[\frac{dC_{L,2}}{d\alpha} \cdot \alpha \cdot \left(1 - \frac{d\varepsilon}{d\alpha} \right) \right] \cdot s_2.$$

FIG. 8 shows a possible lift polar for an arbitrary box wing configuration where the wings have no decalage. Decalage is the difference of the incidence angles of both wings. According to (21) both of the wings are assumed to have the same lift curve slope when isolated. However, the real lift curve slope of the aft wing is lower because of the downwash of the forward wing. The higher the angle of attack, the higher is the difference in lift coefficients. With the help of this simple graph it can already be understood that controlling the aircraft is challenging because of the change of the ratio $C_{L,1}/C_{L,2}$ with angle of attack, since a higher angle of attack means that the forward wing is more loaded than the aft wing. Of course the aircraft can be trimmed for certain angles of attack, but since in the case of the box wing aircraft a whole wing is used for trimming and not a conventional horizontal tail, this could have severe impacts on aircraft performance.

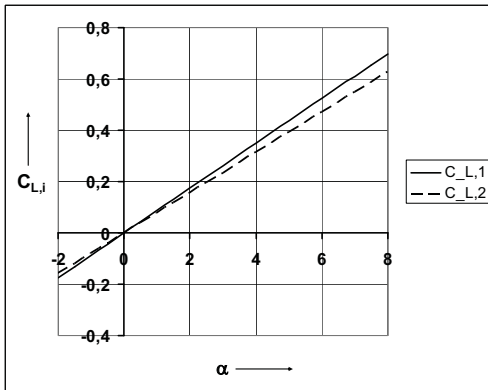


FIG. 8 Generic lift polar of the individual wings of a box wing aircraft

3.5. Maximum Glide Ratio

As it was done with the aerodynamic parameters it is also possible to form the relation of the glide ratios of the reference and the box wing aircraft. The maximum glide ratio of an aircraft is calculated with

$$(27) E_{\max} = \frac{1}{2} \sqrt{\frac{\pi \cdot A \cdot e}{C_{D,0}}}.$$

Based on (2) it is assumed that both the reference and the box wing aircraft have the same aspect ratio. For the current comparison it is also reasonable to suppose that the zero lift drag coefficient of both aircraft is the same as well. In this way the ratio of maximum glide ratios becomes

$$(28) \frac{E_{\max, \text{box}}}{E_{\max, \text{ref}}} = \sqrt{\frac{e_{\text{box}}}{e_{\text{ref}}}}.$$

Applying (15) and taking $D_{i, \text{box}}/D_{i, \text{ref}} = 0,5$ for isolated wings results in a ratio of glide ratios of $\sqrt{2}$, meaning that the theoretical maximum glide ratio of a box wing aircraft is 41 % higher than that of a comparable reference aircraft. Using (20) makes it possible to express the increase of the maximum glide ratio as function of the h/b ratio (FIG. 9).

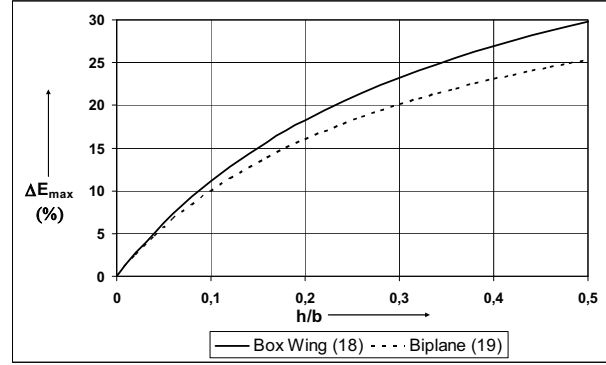


FIG. 9 Possible increase of E_{\max} of a box wing aircraft and a biplane

FIG. 9 shows that for h/b ratios about 0,2, which is a probable value for actual applications, an increase of 17 % of the maximum glide ratio is possible. Note that this number is based on (20) and on the assumption of equal aspect ratios and equal zero lift drag for both the reference and the box wing aircraft. Compressibility is neglected as well.

3.6. Lift Coefficient for Minimum Drag

Based on the idealised quadratic drag polar the lift coefficient for minimum cruise drag is determined to be

$$(29) C_{L, \text{md}} = \sqrt{C_{D,0} \cdot \pi \cdot A \cdot e}.$$

When building the ratio of lift coefficients for minimum drag for the box wing and the reference aircraft and using the same assumptions as in section 3.5 it becomes obvious that the result is the same as for the ratio of maximum glide ratios, hence

$$(30) \frac{(C_{L, \text{md}})_{\text{box}}}{(C_{L, \text{md}})_{\text{ref}}} = \sqrt{\frac{e_{\text{box}}}{e_{\text{ref}}}}.$$

This means that the lift coefficient for minimum drag of the box wing aircraft is higher than that of the reference aircraft.

Supposing that the reference and the box wing aircraft have the same weight, wing area and cruise speed, their wings have to produce the same lift. But for flying with minimum drag they need to operate at different lift coefficients. Taking the lift equation (31) it becomes clear that this is only possible with the help of a different air density, thus a different cruise altitude.

$$(31) L = 0,5 \cdot \rho \cdot v^2 \cdot C_L \cdot S$$

For demonstrating this fact a plot was derived showing the cruise altitude for minimum drag depending on the h/b ratio of the aircraft (FIG. 10). It is based on an aircraft weight of 73,5 t and a cruise Mach number of 0,76. The lift coefficient for minimum drag of the reference aircraft ($h/b = 0$) is 0,71, the wing reference area is 122 m².

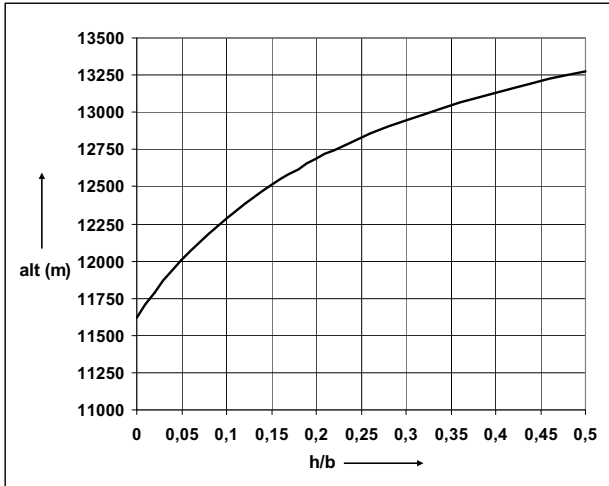


FIG. 10 Altitude for maximum glide ratio as function of the h/b ratio ($m = 73,5$ t; $M = 0,76$, $S = 122\text{m}^2$)

The calculations for producing the plot of FIG. 10 are based on equations for the stratosphere under ISA conditions. For short haul flights it might be inefficient to reach the altitude for maximum glide ratio at all. Flying at such high altitudes requires a heavier fuselage designed for higher cabin pressure differential. In addition flying at high altitudes raises questions concerning ecological effects.

4. SPECIAL CHARACTERISTICS OF THE WING CONFIGURATION

Comparing the reference wing with the box wing configuration it can be stated that the reference wing is split into two wings with half of the chord length of the reference wing. As consequence the airfoil thickness is only about half the thickness of the reference wing. This has significant impacts regarding the wing tank volume and wing structure because of a smaller wing box. These issues are briefly addressed in this section. A more elaborate description of the actual wing design of the medium range box wing aircraft is presented in section 5.2.

An assessment of the effect of lower Reynolds numbers because of smaller chord lengths is part of further studies.

4.1. Wing Tank Volume

Just in the fashion of the previous sections a relation of the wing tank volume of the reference and the box wing aircraft is built. The tank volume of a single wing can be estimated with the following equation, coming from [18]:

$$(32) V_{\text{tank}} = 0,54 \cdot (S_W)^{1,5} \cdot \left(\frac{t}{c}\right)_r \cdot \frac{1}{\sqrt{A}} \cdot \frac{1 + \lambda \cdot \sqrt{\tau} + \lambda^2 \cdot \tau}{(1 + \lambda)^2}$$

with

$$(33) \tau = \frac{(t/c)_t}{(t/c)_r}$$

For this comparison it is reasonable to assume that the wings of both the reference and the box wing aircraft have the same relative airfoil thickness and that the root airfoil has the same relative thickness as the tip airfoil, so that $\tau = 1$ for both wing configurations. Additionally it is supposed that both configurations have the same taper ratio and that the aspect ratio of one single wing of the box wing aircraft is twice the aspect ratio of the reference wing. The area of the reference wing is twice the area of one single wing of the box wing aircraft. Taking account of these conditions and applying (32) gives

$$(34) \frac{(V_{\text{tank}})_{\text{box,iso}}}{(V_{\text{tank}})_{\text{ref}}} = 0,25$$

(34) can also be derived in a simpler way. As mentioned it is assumed that the wing box of one single wing of the box wing aircraft has half the dimensions of the reference wing box, meaning half the chord length/box width and half the box height. Consequently the area of the cross section of the wing box is quarter the area of the reference cross section.

Since the box wing aircraft has two wings, its total wing tank volume is 50 % smaller than the reference wing tank volume, considering the assumptions above.

4.2. Structural Weight

For withstanding the bending moments due to lift a wing box with little height needs a thicker skin which most probably will increase the structural weight. In this section this correlation is examined using an equation for estimating the wing weight proposed in [18]:

$$(35) \frac{m_W}{m_{MZF}} = 6,67 \cdot 10^{-3} \cdot b_S^{0,75} \cdot \left(1 + \sqrt{\frac{b_{\text{ref}}}{b_S}}\right) \cdot n_{\text{ult}}^{0,55} \cdot \left(\frac{b_S/t_r}{m_{MZF}/S_W}\right)^{0,3}$$

Actually (35) applies to conventional cantilever wings, so it cannot be transferred to the box wing configuration without limitations. However the trend of a higher wing weight can already be made out with its help. Using (35) for a box wing aircraft it is assumed that both of its wings can be combined to one conventional reference wing. Like this both the reference and the combined box wings have the same total wing area and the same wing loading m_{MZF}/S_W . The parameters b_s and b_{ref} are the so called structural wing span and another reference wing span (not to confuse with the wing span of the reference aircraft). Both of these parameters are the same for the box wing and the reference aircraft. Assuming an equal maximum zero fuel weight the only parameter which differs for both aircraft is the airfoil thickness at the wing root t_r . So with the help of (35) the following relation can be built:

$$(36) \frac{m_{W,box}}{m_{W,ref}} = \left(\frac{t_{r,ref}}{t_{r,box}} \right)^{0,3} = 2^{0,3} \approx 1,23,$$

meaning that the wing configuration of the box wing aircraft is about 23 % heavier than the reference wing, neglecting the weight of the vertical winglets.

As indicated this number is a rough estimate based on simplifications. The result of a more exact estimation of the wing weight is presented in section 5.2.3.

5. MEDIUM RANGE BOX WING AIRCRAFT

5.1. Main Design Drivers

5.1.1. h/b Ratio

For saving as much induced drag as possible a high h/b ratio is desired (compare FIG. 7). From [2] it can be concluded that ratios of about 0,3 are problematic because of low flutter speeds. Lower ratios seem to increase the speed of flutter onset. For realizing ratios higher than 0,1 it is necessary to have negative stagger so that the aft wing can be connected to the vertical stabilizer. So the design of the vertical stabilizer and the choice of the h/b ratio influence each other.

5.1.2. Static Longitudinal Stability and Controllability

It is intended that the aft wing replaces a conventional horizontal stabilizer for saving wetted area. However, this has drastic consequences regarding static longitudinal stability and controllability. Now the trim condition is hard to accomplish. In general it reads

$$(37) (C_{M,CG})_{C_L=0} > 0,$$

meaning that at zero lift the aircraft must have a positive/nose up pitching moment. Since the zero lift pitching moment of commonly used airfoils is negative there needs to be a component with a sufficient positive zero lift pitching moment. For conventional tail aft aircraft this component is the horizontal tail generating a downward force and thus letting the aircraft pitch up. But for the box wing aircraft both lifting surfaces are supposed to generate positive lift. Here it is more difficult to provide a positive zero lift pitching moment. The consequence is a limited CG envelope and thus the aircraft is very sensitive to shifts of the CG. This is why a well balanced aircraft layout is highly desired.

In [6] and future Aero publications the relations between the requirements of static longitudinal stability and controllability and the CG envelope are further explained. Also different methods of attaining a positive zero lift pitching moment for a box wing aircraft and increasing its CG envelope will be discussed. The most important are

- $C_{L,1} > C_{L,2}$
- huge longitudinal distance between both wings
- adjustments of wing twist and sweep

The approach for the design of the medium range box

wing aircraft is that $C_{L,1} > C_{L,2}$. Since both wings have the same reference area this means that they generate a different amount of lift. According to biplane theory a condition for minimum induced drag is that both wings generate an equal amount of lift. Consequently this condition is not met which leads to an induced drag penalty of about 3 % for the current design.

5.1.3. Fuel Tank Capacity

As outlined in section 4.1 the volume of the wing tanks is significantly smaller than for the reference wing. For fulfilling the reference mission additional tanks are necessary. A part of the additional fuel volume might be provided by a trim tank in the vertical stabilizer. This tank also allows for adjusting the CG position of the aircraft during flight. The rest of the additional volume has to be accommodated with the help of a fuselage tank. Because of the thin wings the center wing box of the forward wing can be located under the cargo floor which makes it possible to have an undivided cargo compartment. In order to retain this nice feature the additional fuselage tank should have the form of a basin which is located below the cargo floor.

5.2. Wing Design

5.2.1. Geometry

Next to the general requirements concerning wing design (transonic speeds, optimum lift distribution, etc.) additional requirements because of the unconventional configuration have to be met. Above all these are the ones coming from static longitudinal stability and controllability. The wing span and the total wing area are the same as for the reference aircraft.

The range for parameters like wing sweep and the t/c ratio is given by transonic aspects. It is desired to have the highest possible t/c ratio so that the wing becomes lighter (compare section 4.2) and has bigger fuel tanks (compare sections 4.1 and 5.1.3). For simplifying the design both wings are supposed to have the same sweep angle, but with opposite directions. The reference aircraft has a sweep angle of 25° . Since both the reference and the box wing aircraft have the same cruise Mach number it could be assumed that the sweep of the box wings might be $25^\circ/-25^\circ$. However, for the desired increase of the t/c ratio a higher sweep is necessary for meeting transonic requirements. It is chosen to be $28,5^\circ/-28^\circ$ which was determined simply by sketching the aircraft and based on additional requirements explained below.

[19] suggests an equation for estimating the maximum allowable t/c ratio depending on the drag divergence Mach number, the wing sweep and the design lift coefficient:

$$(38) \frac{t}{c} = 0,127 \cdot M_{DD}^{-0,204} \cdot \cos\varphi_{25}^{0,573} \cdot C_L^{0,065} \cdot k_M^{0,556}$$

with k_M being a technology parameter having a value of 0,932 for modern supercritical airfoils. The drag divergence Mach number is assumed to be the cruise Mach number ($M = 0,76$) and the wing sweep is given with $28,5^\circ/-28^\circ$. The design lift coefficient is supposed to be the

lift coefficient for minimum drag which is calculated according to (29). The parameters needed for the calculation are the zero lift drag coefficient, the aspect ratio and the span efficiency factor. The aspect ratio of the whole wing configuration is 9,45. The zero lift drag coefficient and the span efficiency factor need to be anticipated from section 5.4.1 ($C_{D,0} = 0,021$; $e = 1,17$). Thus the lift coefficient for minimum drag is 0,84. The resulting maximum allowable t/c ratio is 0,119.

Depending on the sweep angle the taper ratio for a lift distribution close to an elliptical can be determined. [18] proposes

$$(39) \lambda_{opt} = 0,45 \cdot e^{-0,036\phi_{25}}$$

with e being Euler's number. The results are a taper ratio of 0,16 for the forward wing and a ratio of 1,23 for the aft wing. Both of these values are unrealistic. The reference aircraft has a taper ratio of 0,24. This value is chosen for the forward wing. For the aft wing the tip chord length would be higher than the root chord length according to (39). Concerning structures this might cause problems. Taking account of the fixed wing area and for having a sufficient root chord length, e.g. for flap integration, a taper ratio of 0,8 is chosen for the aft wing. Note that (39) actually applies to conventional wings whose loading for minimum induced drag is elliptical. This is not the case for a box wing aircraft, so it is not clear if (39) can be used without limitations.

Now the requirements coming from static longitudinal stability as well as weight and balance (CG position) are taken account of. At first it is intended to place the wings as far apart longitudinally as possible for increasing the CG envelope (compare section 5.1.2). For this the fuselage geometry is required, which can be anticipated from section 5.3.1. For the forward wing the limit is the first door where there should be a clearance of 1 m. The position of the aft wing was chosen so that the sweep of the vertical winglets does not become too high. The position of the overall wing configuration has to comply with the CG of the whole aircraft. This makes it necessary to have a forward swept vertical stabilizer.

For ensuring static lateral stability the forward wing has a dihedral angle of 6°. A dihedral of the upper wing was declined because of structural reasons. The method for determining the dihedral angle can be found in [6].

A summary of the most important geometry parameters is given in Table 1.

TAB 1. Wing geometry parameters

Parameter	Forward wing	Aft wing	Reference wing
Span [m]	34	34	34
Reference Area [m ²]	61	61	122
Aspect ratio	18,9	18,9	9,45
Root chord length [m]	2,9	2	5,9
Taper ratio	0,24	0,8	0,24
Sweep (1/4 chord)	28,5°	-28°	25°
Dihedral	6°	0°	6°

5.2.2. Final Wing Tank Volume

The fuel volume of the designed wing configuration is estimated with the help of (32). All parameters are known except $(t/c)_r$ and τ . For a proper estimation it has to be taken account of the t/c distribution. It is assumed that $(t/c)_r = 0,15$ and that the t/c ratio linearly declines to the value suggested in section 5.2.1, which is 0,119. For the sake of a conservative approach a final value of 0,11 is taken. This value is reached at 35 % half span. For the part of the wing from 35 % half span to the wing tip the t/c ratio is assumed to have a constant value of 0,11. With these data the volume of the wing tanks is as follows:

- Forward: 6,25 m³ (equal to 4,90 t)
- Aft: 5,29 m³ (equal to 4,16 t)

Consequently the total wing tank capacity is about 9,1 t while that of the reference wing tank is 18,7 t.

5.2.3. Wing Weight

As indicated in section 4.2. the wing configuration is heavier than the reference wing. Now the wing weight is estimated in a more exact way based on the actual wing geometry and on the internal loads caused by lift forces. The method of estimation is described and roughly validated in [6]. It is assumed that the wing is only exposed to lift forces at maximum take off mass and a load factor of 3,75 (ultimate load). The lift distribution is supposed to consist of a constant and an elliptical part where the maximum of the elliptical part has the same value as the constant part. The internal loads were determined with the help of a freeware framework tool programmed by G. Wolsink [20]. The weight of a wing is estimated with

$$(40) m_W = 4\rho \left(\frac{1}{0,85 \cdot \epsilon_{all} \cdot E} \cdot \int_0^{b/2} \frac{M(y)}{t(y)} dy + \frac{1}{2 \cdot \gamma_{all} \cdot G} \cdot \int_0^{b/2} S_L(y) dy \right)$$

(40) was derived with the help of the approach for wing weight estimation presented in [21]. The wing weight is estimated only with the help of the distribution of bending moments and shear forces. The material properties are those of aluminium. The resulting weights are as follows:

- Forward wing: 6,7 t
- Aft wing: 5,0 t

Note that the weight of the winglets is not included yet. Currently it is approximated to be 1 t in total. Thus the resulting weight of the whole wing configuration is 12,7 t. This is about twice as heavy as the reference wing which indicates that the estimation according to (36) is too optimistic.

5.2.4. High Lift

A detailed investigation concerning high lift has yet to be made. However some important aspects can already be mentioned. As described in section 5.1.2 the lift coefficient of the forward wing needs to be higher than that of the aft wing because of static longitudinal stability. For cruise flight with maximum take off mass the ratio $C_{L,1}/C_{L,2}$ is determined to be 1,74 [6]. Assuming a maximum lift coefficient of about 2,95 for the whole aircraft and taking the ratio of 1,74 for landing, this would mean that the lift

coefficient of the forward wing has a value of 3,75 which is quite unrealistic. Consequently the layout of the high lift devices becomes difficult. One option could be to increase the landing field length of the aircraft. This way a lower maximum lift coefficient is required. On the other hand the total wing area could be increased for lowering the required lift coefficients. The ratio $C_{L,1}/C_{L,2}$ still has to be investigated for other flight phases than cruise.

5.3. Design of Other Components

5.3.1. Cabin and Fuselage

The characteristics according to static longitudinal stability and controllability require the CG travel to be minimized. This is why the cabin is designed as compact as possible, meaning that its length is shortened compared to the reference cabin. For accommodating the same number of passengers as the reference aircraft this requires a higher number of seats abreast, which is chosen to be eight. Consequently the cabin has two main aisles.

The fuselage layout was performed with PreSTo Cabin [22]. The resulting circular cross sections for business and economy class are shown in FIG. 11, the main cabin and fuselage parameters in Table 2.

For assuring equal payload-range characteristics as the reference aircraft the additional fuselage tank is supposed to have a volume of about 8,6 m³, which equals a fuel mass of 6,7 t. Depending on the final height of the fuel basin its length is about 3 m.

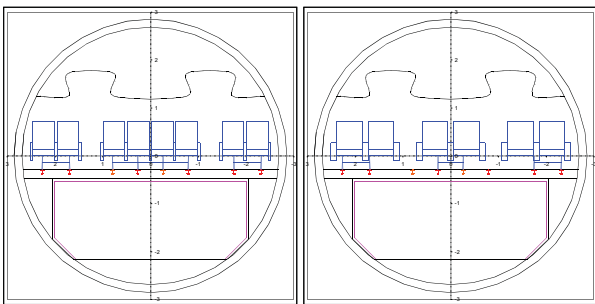


FIG. 11 Fuselage cross sections for economy (left) and business class (right)

TAB 2. Cabin and fuselage properties

Fuselage length [m]	33,1
Fuselage diameter [m]	5,7
Fuselage fineness ratio	5,8
Fuel tank capacity [t]	6,7
Cargo volume [m ³]	43 (12x LD3)
Cabin length [m]	21,9
B/C	12 pax, 2-2-2, 36" seat pitch
Y/C	138 pax, 2-4-2, 32" seat pitch

5.3.2. Empennage

A V-tail is chosen for increasing the stability of the aft wing. As stated in section 5.1.2 the aft wing is supposed to include the functions of a horizontal stabilizer. This is why the size of the V-tail is determined according to the

requirements for a vertical stabilizer. For roughly sizing the V-tail a simple approach based on the vertical tail volume is chosen. It is given by

$$(41) V_V = S_V \cdot l_V \cdot$$

The vertical tail volume of the box wing aircraft is supposed to be the same as for the reference aircraft. Based on the geometry of the reference aircraft its vertical tail volume is determined to be about 300 m³ where S_V is about 19,5 m² and l_V about 15,5 m. From the final aircraft layout the lever arm l_V is determined to be about 12 m for the box wing aircraft. According to (41) the required tail surface is 25 m². Since the tail consists of two surfaces, the area of one individual surface consequently is 12,5 m². Note that this number refers to the projected area of one surface, since they are actually angular. Now the remaining geometry parameters of the surfaces have to be determined. For this the equation for calculating the surface of a trapeze is used which, applied to the projected area of one tail surface, reads

$$(42) S_V = 0,5 \cdot (c_{r,V} + c_{t,V}) \cdot h_V \cdot$$

The chord length at the tip is supposed to be the chord length of the aft wing so that there is a smooth junction. The relating chord length is 1,9 m. The height is chosen so that the h/b ratio does not significantly exceed a value of 0,2 because of expected flutter requirements. According to [23] the aspect ratio of a vertical stabilizer should range from 0,7 to 2. This also influences the height. Finally a stabilizer height of 3,4 m is chosen which results in a h/b ratio of 0,22 and a projected aspect ratio of 1,5. Now the chord length at the stabilizer root can be calculated with the help of (42), resulting in a length of 3,8 m. Consequently the stabilizer taper ratio is 0,5, which is within the range proposed by [23] (0,26 to 0,73). At last the sweep angle has to be set. According to [23] it is supposed to be within 33° and 53° for jet transport aircraft. The stabilizer is connected to the aft wing and the balanced aircraft configuration requires the whole wing configuration to be almost in the middle of the fuselage. For providing enough sweep of the V-tail, it has to be swept forward as consequence. The chosen sweep angle is -30°.

The final geometry of the tail surfaces is shown in FIG. 12. The relating geometry parameters are summarized in Table 3.

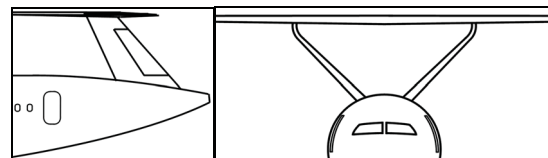


FIG. 12 Side and front view of the V-tail

TAB 3. Geometry of the V-tail

Projected area (single stabilizer) [m ²]	12,25
Stabilizer height [m]	4,3
Projected aspect ratio (single stabilizer)	1,51
Root chord length [m]	3,8
Tip chord length [m]	1,9
Taper ratio	0,5
Sweep angle (1/4 chord)	-30°
Lever arm [m]	12
Total tail volume [m ³]	294

5.3.3. Engines

Because of the aircraft's sensitivity to CG shifts the engines have to be positioned close to the CG so that its shift is minimal when loading the aircraft. The wing positions are not suitable for placing the engines on the wings and meeting this requirement. This is why the engines are positioned in the middle of the fuselage. The way of engine integration is shown in FIG. 13.

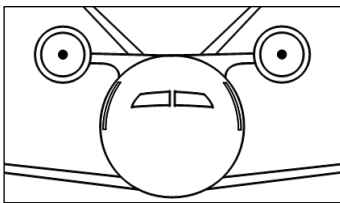


FIG. 13 Engine integration

The engines are carried by a beam which goes through the upper side of the fuselage. The structural design of this option might become critical because the beam intrudes the pressure hull of the fuselage. Another possibility is placing the beam outside of the fuselage, comparable to the wing integration of the ATR 42/72. This might however increase drag. For integrating engines with higher bypass ratios, and thus higher diameters, the span of the beam can be increased.

5.3.4. Landing Gear

An integration of the main landing gear into the wing, as applied for conventional configurations, is not possible for the box wing aircraft because of the unsuitable wing positions. So an integration into the fuselage comparable to the Avro RJ has to be applied. For the current design of the medium range box wing aircraft the layout of the landing gear only comprises aspects concerning sufficient ground clearance and tip over stability. The design of actual mechanical components is not part of the current process.

The position of the main landing gear is chosen so that a tail strike is avoided during take off rotation. It also has to provide enough clearance in the case of unexpected rolling maneuvers during landing or take off. FIG. 14 and FIG. 15 show that these requirements are taken account of.

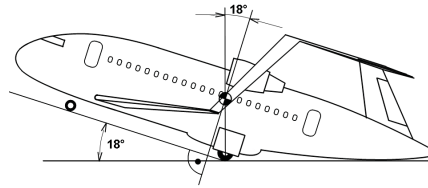


FIG. 14 Pitch angle at tail strike

According to [24] the pitch angle at tail strike should be within the range from 8° to 13°. The main gear position relative to the CG is expressed with the help of an angle (see FIG. 14). According to [25] the minimum value of this angle is 15° so that a sufficient pitch down moment is induced during landing. For sufficient tip over stability this angle shall at least have the value of the pitch angle at tail strike [25]. It has to be noted that the vertical position of the CG is guessed at this stage of the investigation.

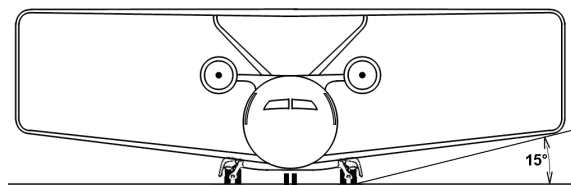


FIG. 15 Wing clearance to ground

[24] states that the angle indicated in FIG. 15 has to be at least within the range from 6° to 8°.

Longitudinal tip over stability can be assessed with the help of the relating tip over angle (FIG. 16). The requirement is a tip over angle of less than 55°. The necessary coordinates for the determination of the tip over angle and the result are given in Table 4. The calculation itself can be found in [6]. Consequently the gear position was properly chosen for complying with the requirements according to longitudinal tip over stability.

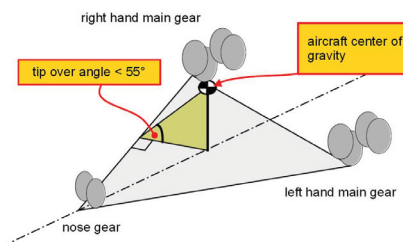


FIG. 16 Tip over angle (acc. to [24])

TAB 4. Input parameters and result of tip over angle calculation

	Coordinates [m]		
	x	y	z
Center of gravity	16,4	0	4,7
Nose gear	5,2	0	0
Main gear (right)	17,7	4	0
Tip over angle	54°		

5.4. Performance and Weight

5.4.1. Final Maximum Glide Ratio

In order to determine the final maximum glide ratio with the help of (27) the zero lift drag coefficient of the aircraft and its span efficiency factor need to be known. The first is estimated with the help of the relative wetted area, the latter is calculated according to (20). The zero lift drag coefficient depending on the relative wetted area is given with

$$(43) C_{D,0} = C_{fe} \cdot \frac{S_{wet}}{S_W}$$

where the skin friction coefficient is estimated to be 0,003. For the box wing aircraft the relative wetted area is determined to be 7,0. The relating calculations are presented in [6] and future Aero publications. The resulting zero lift drag coefficient is 0,021.

For a *h/b* ratio of 0,22 and according to (20) with $e_{ref} = 0,85$ the span efficiency factor of the box wing aircraft is 1,17. This includes a 3 % induced drag penalty because of the unequal lift of both wings.

According to (27) the maximum glide ratio is 20,4. In relation to the reference glide ratio of 17,9 this means a 14 % increase. According to (28) a maximum glide ratio of 21,0 would be expected (17 % increase). This number is reduced since the reference zero lift drag is assumed to be 0,02, which is lower than that of the box wing aircraft.

5.4.2. Weight Breakdown

Table 5 shows a comparison of the operating empty weight, the maximum zero fuel weight and the maximum take off weight of the reference and the box wing aircraft. The method of weight estimation is mostly based on the proposals in [18] and the details are presented in [6] as well as in future Aero publications.

TAB 5. Weight comparison of the reference and the box wing aircraft

	Box Wing	Reference	Deviation
m_{OE} [kg]	41333	40500	2,2 %
m_{MZF} [kg]	61333	60500	1,4 %
m_{MTO} [kg]	73500	73501	0,0 %

It is astonishing that both aircraft have the same maximum take off weight. The operating empty weight of the box wing aircraft is higher because of the heavy wing configuration. However, the weight penalty because of the wing configuration is partly compensated by a lighter fuselage, which is shown in FIG. 17. FIG. 17 is based on the reference mission and shows that the box wing consumes about 9 % less fuel.

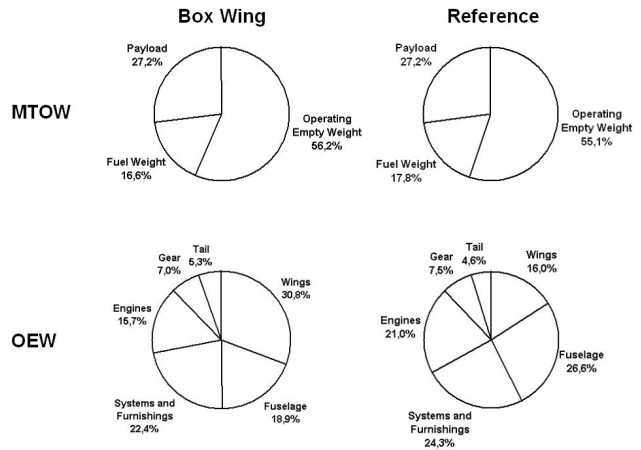


FIG. 17 Weight breakdown of the box wing and the reference aircraft

5.4.3. Payload-Range Diagram

The payload-range diagrams of both the reference and the box wing aircraft are determined with the help of the Breguet range equation. In this section only the relating input parameters and results are presented. The detailed calculation can be found in [6].

At first the fuel capacity of both aircraft is required. The reference aircraft stores all of the fuel inside the wing tanks whose capacity is 18,7 t. The capacity of the box wing aircraft includes the wing tanks (9,1 t), the fuselage tank (6,7 t) and the trim tank (1 t) giving a total of 16,8 t. With the help of these capacities and the available performance data the following results are calculated (Table 6).

TAB 6. Results of the payload-range calculations

	Box Wing		Reference	
	Payload	Range	Payload	Range
Max payload	20 t	2870 km	20 t	2870 km
Max fuel	15,4 t	5247 km	14,4 t	5313 km
Ferry range	0 t	7580 km	0 t	7480 km

The payload-range characteristics of both aircraft are comparable. But the box wing has the advantage of a lower fuel consumption. This also means that it is able to carry a higher payload when its tanks are completely full. FIG. 18 shows the payload-range diagram.

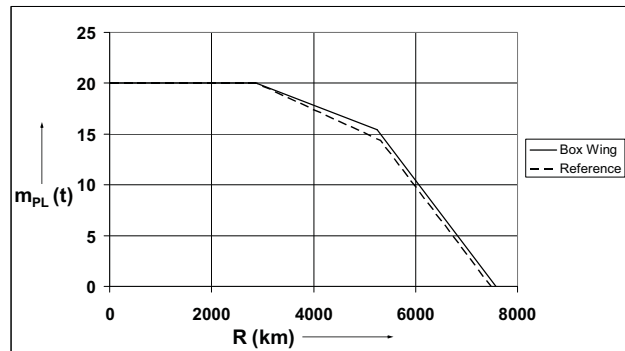


FIG. 18 Payload-range diagram

5.5. Family Concept

The development of a new commercial aircraft commonly does not only include one basic aircraft but also stretched and shrunk versions so that the aircraft manufacturer is able to cover several market segments with this aircraft. The absence of this possibility is most probably a reason for abandoning the affected aircraft program. This is why the possibility of stretching or shrinking the medium range box wing aircraft is essential for its existence.

Usually the fuselage length of a basic aircraft version is changed by inserting/removing fuselage sections in front and aft of the wing so that the balance of the aircraft is kept. In this way the wing configuration does not need to be changed. For the box wing aircraft this approach is not feasible since the aft wing is attached to the empennage. So the only way of changing the fuselage length is to insert/remove fuselage sections between the forward and the aft wing, ideally one in front and one aft of the engines. However, this also changes the distance between the forward and the aft wing. Since their geometry is desired to be unchanged a redesign of the vertical winglets is necessary because they now have a different sweep. A comparison of the basic box wing aircraft and a possible stretched version is shown in FIG. 19.

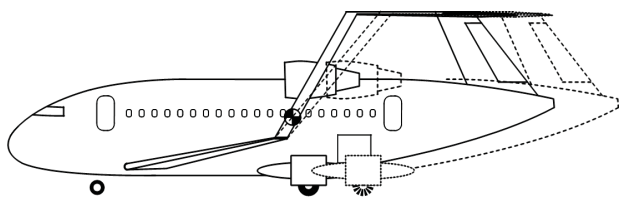


FIG. 19 Comparison of the basic box wing aircraft and a possible stretched version.

It is important to note that the resulting change of stagger influences the lift distribution of both wings which then deviates from the optimum. Consequently the span efficiency factor for a stretched/shrunk version is decreased. The magnitude of this efficiency loss has not been assessed yet.

6. CONCLUSION

The aim of this paper was to define the geometry of the wing configuration of a box wing aircraft and to describe fundamentals of box wing aerodynamics and flight mechanics with the help of these definitions in the perspective of aircraft design. This allows for properly designing a medium range box wing aircraft.

Concerning the geometry of the wing configuration the aspect ratio was defined. Here a distinction between the aspect ratio of a single wing and that of the whole wing configuration needs to be made. Based on this differentiation the savings in induced drag can be justified either in the one or the other way. It was concluded that the approach considering the whole wing configuration is the most suitable because in this way it is possible to determine the span efficiency of the aircraft with the help of literature data. Considering the vertical gap it was emphasized that the distance at the wing tips is crucial for

the span efficiency. Thus the h/b ratio of the medium range box wing aircraft is defined to be h/b . However, the possibility of using an average h/b ratio for a wing configuration where both wings have different dihedral was not explored yet.

Based on the span efficiency general considerations about box wing performance were made. It was shown that for reaching the maximum glide ratio the box wing aircraft has to fly at higher altitudes, provided that it has the same weight and cruise speed as the reference aircraft.

In a short section it was shown why the wing configuration of the box wing aircraft has a smaller fuel volume and a higher weight than the reference wing. From these facts the need for a higher t/c ratio is reasoned. For meeting the requirements of transonic flight the sweep of the designed medium range box wing aircraft is chosen to be higher than that of the reference aircraft. In this way an increase of the t/c ratio is realizable. It was shown that there is great interaction between wing design and the layout of the fuselage and the empennage in contrast to conventional aircraft. The whole aircraft is designed so that the CG shift for all flight scenarios is minimal. This is necessary because of the relatively small CG envelope of the designed box wing aircraft. Consequently the cabin is shorter than the reference cabin and the engines are placed in the middle of the fuselage. The main landing gear has to be integrated within the fuselage as well. Its position was chosen to assure sufficient ground clearance and tip over stability. Because of the low fuel capacity of the wings an additional fuselage tank is necessary. It is proposed to be a basin situated below the cargo floor, so that there is the possibility of an undivided cargo compartment.

The maximum take off weight of the box wing aircraft was found to be equal to that of the reference aircraft. The final weight of the wing configuration was estimated to be twice as heavy as the reference wing. This weight penalty can be compensated by less required fuel and a lower fuselage weight. Finally the box wing aircraft consumes 9 % less fuel for the reference mission because of its higher glide ratio (14 % increase compared to the reference aircraft). With the help of the additional fuselage tank the payload-range characteristics of the box wing aircraft are comparable to those of the reference aircraft. The realization of a box wing aircraft family concept includes some critical points. The most important one is the change of stagger which also changes the lift distribution of the wings.

It has to be pointed out that the present design of the box wing aircraft only shows the fundamental investigation. The negligence of wave drag is compensated by using an equation producing lower values for the span efficiency of the aircraft than in other comparable studies. An in depth analysis of flight mechanics, especially concerning static longitudinal stability and controllability, is shown in [6] and future Aero publications. The layout of control surfaces and high lift devices is still open. A more detailed analysis of aerodynamics, flight dynamics and other relevant disciplines has yet to be made.

ACKNOWLEDGEMENT

The project underlying this report was funded by the German Federal Ministry for Education and Research (support code (FKZ) 03CL01G). The authors are responsible for the content of this publication.

NOMENCLATURE

Symbols

A	aspect ratio
b	wing span
c	chord length
\bar{c}	mean aerodynamic chord length
C	coefficient for total aircraft
CO_2	carbon dioxide
D	drag
e	span efficiency factor
E	glide ratio, Young's modulus
G	shear modulus
h	height, vertical gap
k	free parameter
l	lever arm
L	lift
m	mass
M	moment, Mach number
n	load factor
NO_x	nitrogen oxide
q	dynamic pressure
s	relative wing reference area
S	wing reference area, shear load
t	airfoil thickness
v	velocity
V	volume
x	longitudinal position
α	angle of attack
γ	shear strain
ε	downwash, normal strain
λ	taper ratio
ρ	density
τ	airfoil thickness ratio (tip to root)
φ	sweep angle

Indices

0	zero lift
25	quarter chord
50	half chord
all	allowed
bi	biplane
box	box wing aircraft
CG	center of gravity
CG-AC	from center of gravity to aerodynamic center
cr	cruise
DD	drag divergence
fe	skin friction
i	induced
iso	isolated
max	maximum
M	material/technology
md	minimum drag
MTO	maximum take off
MZF	maximum zero fuel

OE	operating empty
opt	optimum
r	wing root
ref	reference
S	structural
t	wing tip
tank	fuel tank
tot	total
ult	ultimate
V	vertical tail
W	wing
wet	wetted

Abbreviations

CFD	computational fluid dynamics
CG	center of gravity
MAC	mean aerodynamic chord
MTOW	maximum take off weight
OEW	operating empty weight
PreSTo	aircraft preliminary sizing tool
VLM	vortex lattice method

LIST OF REFERENCES

- [1] EUROPEAN COMMISSION: *Flightpath 2050 : Europe's Vision for Aviation*. Luxembourg, Publications Office of the European Union, 2011.
- [2] LANGE, R.H. ; CAHILL, J.F. ; BRADLEY, E.S. ; et al.: *Feasibility Study of the Transonic Biplane Concept for Transport Aircraft Application*. Marietta : The Lockheed-Georgia Company, 1974. - Research report prepared under contract NAS1-12413 on behalf of the National Aeronautics and Space Administration
- [3] <http://Airport2030.ProfScholz.de/> (2011-08-01)
- [4] PESTER, Maria: *Multi-Disciplinary Conceptual Aircraft Design Using CEASIOM*. Hamburg, Hamburg University of Applied Sciences, Department of Automotive and Aeronautical Engineering, Master Thesis, 2010
- [5] KHAN, Fahad A.; KRAMMER, Philip; SCHOLZ Dieter: Preliminary Aerodynamic Investigation of Box-Wing Configurations Using Low Fidelity Codes. In: DGLR: *Deutscher Luft- und Raumfahrtkongress 2010 : Tagungsband – Manuskripte* (DLRK, Hamburg, 31. August – 02. September 2010). – ISBN: 978-3-932182-68-5. DocumentID: 161308
- [6] SCHIKTANZ, Daniel: *Conceptual Design of a Medium Range Box Wing Aircraft*. Hamburg, Hamburg University of Applied Sciences, Department of Automotive and Aeronautical Engineering, Master Thesis, 2011.
- [7] KROO, Ilan: Drag due to Lift : Concepts for Prediction and Reduction. In: *Annual Review of Fluid Mechanics Vol. 33* (2001), p. 587-617

- [8] DURAND, William F. (Ed.); VON KÁRMÁN, Theodore; BURGERS, J.M.: *Aerodynamic Theory Vol. 2 : General Aerodynamic Theory – Perfect Fluids*. Berlin : Julius Springer, 1935
- [9] FREDIANI, Aldo; MONTANARI, Guido: Best Wing System: An Exact Solution of the Prandtl's Problem. In: BUTTAZZO, Giuseppe (Ed.); FREDIANI, Aldo (Ed.): *Variational Analysis and Aerospace Engineering*. Dordrecht, Heidelberg, London, New York : Springer, 2009, p. 183-211.- ISSN 1931-6828, ISBN 978-0-387-95856-9, e-ISBN 978-0-387-95857-6
- [10] FREDIANI, Aldo : The Prandtl Wing. In: VON KÁRMÁN INSTITUTE FOR FLUID DYNAMICS: *VKI Lecture Series : Innovative Configurations and Advanced Concepts for Future Civil Transport Aircraft*. Rhode St-Genève: Von Kármán Institute for Fluid Dynamics, 2005
- [11] KROO, Ilan : Nonplanar Wing Concepts for Increased Aircraft Efficiency. In: VON KÁRMÁN INSTITUTE FOR FLUID DYNAMICS: *VKI Lecture Series : Innovative Configurations and Advanced Concepts for Future Civil Transport Aircraft*. Rhode St-Genève: Von Kármán Institute for Fluid Dynamics, 2005
- [12] DEMASI, Luciano: Investigation on Conditions of Minimum Induced Drag of Closed Wing Systems and C-Wings. In: *Journal of Aircraft Vol. 44 (1/2007)*, p. 81-99
- [13] PRANDTL, Ludwig: *Induced Drag of Multiplanes*. Hampton : National Advisory Committee for Aeronautics, 1924. - NACA TN 182
- [14] RIZZO, Emanuele: *Optimization Methods Applied to the Preliminary Design of Innovative, Non Conventional Aircraft Configurations*. Edizioni ETS. Pisa, 2007.- ISBN 978-884672458-8
- [15] SCHOLZ, Dieter: *Skript zur Vorlesung Flugzeugentwurf*, Hamburg, Fachhochschule Hamburg, FB Fahrzeugtechnik, Abt. Flugzeugbau, Aircraft Design Lecture Notes, 1999
- [16] FINCK, R. D.: *USAF Stability and Control Datcom*. Long Beach (CA) : McDonnell Douglas Corporation, Douglas Aircraft Division, 1978. - Report prepared under contract F33615-76-C-3061 on behalf of the Air Force Wright Aeronautical Laboratories, Flight Dynamics Laboratory, Wright-Patterson AFB (OH)
- [17] GALL, Peter D.: *An Experimental and Theoretical Analysis of the Aerodynamic Characteristics of a Biplane-Winglet Configuration*. Hampton : National Aeronautics and Space Administration, 1984. - NASA TM 85815
- [18] TORENBEEK, Egbert: *Synthesis of Subsonic Airplane Design*. Delft : Delft University Press, 1982. - ISBN 90-247-2724-3
- [19] SCHOLZ, Dieter; CIORNEI, Simona: Mach number, relative thickness, sweep and lift coefficient of the wing – An empirical investigation of parameters and equations, (Deutscher Luft- und Raumfahrtkongress, Friedrichshafen, 26. – 29. September 2005). In: BRANDT, P. (Ed.): *Jahrbuch 2005*. Bonn : Deutsche Gesellschaft für Luft- und Raumfahrt, 2005. – Paper : DGLR-2005-122, ISSN 0070-4083
- [20] <http://members.ziggo.nl/wolsink/> (2011-06-28)
- [21] OYAMA, Akira: Multidisciplinary Optimization of Transonic Wing Design Based on Evolutionary Algorithms Coupled With CFD Solver. In: ECCOMAS: *European Congress on Computational Methods in Applied Sciences and Engineering* (Barcelona, 11-14 September 2000)
- [22] <http://PreSTo.ProfScholz.de> (2011-08-01)
- [23] ROSKAM, Jan: *Airplane Design : Part II: Preliminary Configuration Design and Integration of the Propulsion System*. Kansas : Roskam Aviation and Engineering Corporation, 1985
- [24] TRAHMER, Bernd: *Fahrwerk / Undercarriage / Landing Gear : Fahrwerksintegration in den Gesamtentwurf*. Hamburg, University of Applied Sciences Hamburg, Department of Automotive and Aeronautical Engineering, Lecture Notes, 2004
- [25] ROSKAM, Jan: *Airplane Design : Part IV: Layout Design of Landing Gear and Systems*. Kansas : Roskam Aviation and Engineering Corporation, 1985